Soil load support capacity increases with time without soil mobilization as a result of age-hardening phenomenon

Moacir Tuzzin de Moraes[a,*], Felipe Bonini da Luz[b], Henrique Debiasi[c], Julio Cezar Franchini[c], Vanderlei Rodrigues da Silva[b]

[a] *University of Sao Paulo, 13416-000, Piracicaba, SP, Brazil*
[b] *Federal University of Santa Maria, 98400-000, Frederico Westphalen, RS, Brazil*
[c] *Embrapa Soja, PO Box 231, 86001-970, Londrina, PR, Brazil*

ARTICLE INFO

ABSTRACT

Soil compaction is a result of soil compression, and this effect depends on the pressure applied and the soil structure. Nevertheless, studies regarding the effects of long-term tillage systems on strengthening of particle bonds are scarce. Thus, we aimed to study the soil bond strengthening due to the age-hardening phenomenon using the soil load support capacity model of an Oxisol managed under different tillage systems in Southern Brazil. Soil samples were collected from three soil layers (0.0–0.10 m; 0.10–0.20 m and 0.20–0.30 m) and five soil tillage systems of conventional tillage; minimum tillage with chiselling performed every year or every three years; and no-tillage for 11 or 24 years. Age-hardening was investigated using the soil load support capacity model. Soil cores were equilibrated at four matric potentials (-6, -33, -100 and -500 kPa) and submitted to uniaxial compression tests to obtain preconsolidation pressure. The soil load support capacity models were affected by the tillage systems. The long-term no-tillage presented the highest soil load support capacity for the same bulk density and water content in all layers, demonstrating greater resistance to additional compaction. Higher preconsolidation pressure values in long-term no-tillage at the same soil bulk density and water content were attributed to the age-hardening phenomena, which increased the number and strength of bonds among soil particles, leading to higher soil cohesion. Longer time under no-tillage improves the soil structure and soil load support capacity. Thus, soil mobilization strongly affected the soil structure by breaking particle bonds leading to the greater compaction.

1. Introduction

Soil load support capacity has been known as a tool to evaluate soil structure and management in mechanized areas (Keller and Lamandé, 2010). This parameter is determined from the precompression stress (σ_p), which indicates the maximum load pressure applicable to the soil without additional compaction (Dias Junior and Pierce, 1995), and it has been used as a soil physical quality indicator (Imhoff et al., 2016).

Soil load support capacity is affected by several soil attributes, e.g., organic matter content, texture, type and concentration of iron oxides (Mazurana et al., 2017), water content (Tang et al., 2009), bulk density (Assouline, 2002), porosity (Veiga et al., 2007), structure (Veenhof and McBride, 1996), and especially the cohesion and adhesion forces among soil particles (Horn, 2004). However, soil load support capacity has rarely been related to soil strengthening resulting from the age-

hardening process (Moraes et al., 2017).

Age-hardening is described as the process through which soil strength increases spontaneously over time after soil disturbance by the greater bonding and cementation among soil particles (Dexter et al., 1988; Moraes et al., 2017; Utomo and Dexter, 1981). Two different mechanisms are involved in the age-hardening called type A and type B (Dexter et al., 1988; Moraes et al., 2017). Type A age-hardening occurs when new bonds are formed by the rearrangement of soil particles into new positions of minimum free energy. In the type B mechanism, existing bonds among soil particles become stronger. Additionally, the critical water content for the type B mechanism increases as a function of the soil organic carbon content (Utomo and Dexter, 1981).

Most soil properties associated with σ_p and hence, with soil load support capacity, are influenced by cropping and soil tillage systems (Moraes et al., 2017; Ortigara et al., 2015; Pires et al., 2017).

Nevertheless, studies regarding the effects of long-term tillage systems on age-hardening are scarce (e.g., Moraes et al., 2017), and mainly focused on clayey soils in subtropical regions and even less information can be found concerning tillage effects on soil load support capacity in response to the age-hardening. Such knowledge is of particular interest in Southern Brazil, where soil chiselling rather than biological practices (e.g., crop rotation) has been increasingly adopted by soybean producers to mitigate soil compaction in areas managed under no-tillage (Franchini et al., 2012). In this sense, soil disturbance caused by chiselling is known to disrupt soil aggregates and bonds among soil particles (Nunes et al., 2015; Silva et al., 2014), which in turn may revert the age-hardening effects provided by long-term no-tillage (Moraes et al., 2017). Hence, reduced soil load support capacity is expected, leading to the higher compaction risks in chiselled areas.

We hypothesised that avoiding soil disturbance (no-tillage system) increases soil load support capacity under the same bulk density and water content over time as a result of the age-hardening process. We aimed to study the soil strengthening due to the age-hardening phenomenon using the soil load support capacity model of an Oxisol managed under different tillage systems in Southern Brazil.

2. Material and methods

2.1. Study site

The study was carried out in a long-term experiment, implemented in the summer of the 1988/1989 crop season, at the Experimental Station of Embrapa Soja, in Londrina (latitude 23°11′S; longitude 51°11′W; and altitude of 620 m asl), State of Paraná, Southern Brazil. According to the Köppen classification, the climate is humid subtropical (Cfa), with annual average temperature of 20.3 °C (Alvares et al., 2013). The mean annual precipitation is 1575 mm, with mean of 207 mm, in December (the wettest month); and 62 mm, in August (the driest month) (Alvares et al., 2013). The experiment was established in an Oxisol (Latossolo Vermelho Distroférrico, Brazilian classification (Santos et al., 2013) or Rhodic Eutrudox, USA classification (Soil Survey Staff, 2014)) with 755 g kg^{-1} of clay, 178 g kg^{-1} of silt, and 67 g kg^{-1} of sand. The soil particle density at 0-0.3 m depth is 2.90 Mg m^{-3}, and the mean slope of the experimental area is 0.03 m m^{-1}. In the 1940s, the native forest was converted to agriculture. The area had been cultivated with coffee (*Coffea arabica* L.) from 1950 to 1976 under conventional management (only with hoeing and cutting of weeds in the inter-row). From 1976 to 1986 the area was under annual cropping in succession of soybean-wheat under conventional tillage system (with mouldboard plough and heavy disking). The trial was established in the summer of 1988/1989 crop season, when this experiment was initiated. Before the establishment of the experiment, the entire area was managed similarly in terms of soil tillage, cropping system and fertilizer inputs.

2.2. Experimental design, treatments, and field management

The experiment was laid out in a 5 × 2 factorial arrangement (soil tillage x cropping system), distributed in a randomised block design with four replications. The following tillage systems were evaluated: conventional tillage with heavy disking to a depth of 0.15 m, then light disking (0.10 m depth), performed before each winter and summer growing season (CT); minimum tillage with annual chiselling (0.30 m depth), performed before each winter crop planting, and no-tillage for the summer crop (MTC$_1$); minimum tillage with chiselling every three years (0.30 m depth), performed before the winter crop planting, and no-tillage for the summer crops (MTC$_3$); continuous no-tillage for 11 years, established in 2001 (NT$_{11}$); and continuous no-tillage for 24 years (NT$_{24}$), established in 1988. Between 1988 and 2001, the soil under NT$_{11}$ was tilled with a mouldboard plough (average working depth of 0.32 m), followed by light disking before planting the summer

crop, and heavy disking (average working depth of 0.15 m) followed by light disking (0.07 m working depth) before the planting of the winter crop. The MTC$_1$ and MTC$_3$ plots were chiselled using a mounted, tractor-pulled chisel plough with rollers and four shanks spaced 0.40 m apart, working at an average depth of 0.30 m and an angle of 45°.

The soil tillage systems were performed under two different cropping systems: (i) wheat (*Triticum aestivum* L.) in the winter, and soybean (*Glycine max* (L.) Merr.) in the summer every year (crop succession); and (ii) a four-year crop rotation system, with the following species (winter/summer): year 1 = white lupine (*Lupinus albus* L.) or radish (*Raphanus sativus* L.)/maize (*Zea mays* L.); year 2 = white oat (*Avena strigosa* Schreb.)/soybean; year 3 = wheat/soybean; and year 4 = wheat/soybean (crop rotation). Each plot was 30 m long × 10 m wide (area of 300 m^2), with 7 m distance between them to allow tractor manoeuvring during operations. The average shoot dry biomass production of the plant species in crop succession and rotation systems was approximately 5.3 and 7 Mg ha^{-1} yr^{-1}, respectively. More details about the experiment can be found in Moraes et al. (2016).

2.3. Soil sampling and laboratory analysis

Soil sampling was carried out in January 2012, at the R3 phenological growth stage of soybean crop, after 10 and 22 months from the last soil chiselling in MTC$_1$ and MTC$_3$, respectively. Soil cores were collected from the centre of three layers (0.0-0.10, 0.10-0.20, and 0.20-0.30 m depth) using stainless steel rings (6.3 cm internal diameter, 2.5 cm height, and 78 cm^3 internal volume). Considering the factorial design, 10 treatments were established (5 tillage systems x 2 cropping systems) with 4 replications and 3 soil layers. Considering three soil samples in each treatment, replicate, and soil layer, the total of 360 soil samples were collected from the soybean inter-rows. The samples were divided into four groups of 90, each group containing samples of all the possible treatments. After being saturated by capillarity, each group was subjected to the following soil matric potentials: −6 kPa using suction tables; and −33 kPa, −100 kPa, and −500 kPa in Richards' chambers with porous plates.

Once equilibrated at the respective matric potentials, the samples were weighed, and subjected to the uniaxial compression test using a pneumatic, all-automatic consolidometer (Model: CNTA-IHM / BR-001/07). In the uniaxial compression test, the soil cores were subjected to the pressures of 25, 50, 100, 200, 400, 800 and 1600 kPa (Silva et al., 2007) and the displacement at each of the pressures applied was recorded. Each sample was under pressure for 5 min which is enough to obtain 99% of the maximum strain (Silva et al., 2000). After the uniaxial compression test, the soil cores were oven-dried at 105 °C for 48 h to quantify the soil bulk density (BD) and gravimetric soil water content (W). The bulk density was obtained based on dry mass and soil volume calculated from the strain recorded for each pressure applied. The bulk density before pressure application was determined from the dry mass and the core volume (Blake and Hartge, 1986a). The soil particle density (PD) was quantified using the volumetric flask method (Blake and Hartge, 1986b), and the void ratio (ε) was calculated for the soil sample after each compression according to the Eq. (1).

$$\varepsilon = \left(\frac{PD}{BD}\right) - 1 \tag{1}$$

Where ε is the void ratio, PD is the particle density (m^3 m^{-3}), and BD is the soil bulk density (Mg m^{-3}).

The soil compression curve was plotted for each soil core, using the logarithm (base 10) of the applied stress (*x-axis*) and the void ratio (*y-axis*). The σ_p was obtained from the compression curve using the Casagrande (1936) method, mathematically operationalized with the equation of van Genuchten (1980), as described in Baumgartl and Kock (2004) (Eg. 2). The Soil Compression Curve Excel® Add-in (SCC) developed by Gubiani et al. (2017) was used to fitting the parameters in Eq. (2) and calculating σ_p, as described in the software. In the fitting

routine, the software SCC also converts the $\varepsilon-\sigma_P$ relationship to the $\varepsilon-log_{10}\sigma_P$ relationship, which is the classic compression curve shape ($\varepsilon-log_{10}\sigma_P CC$) (Gubiani et al., 2017).

$$\varepsilon = \varepsilon_f + (\varepsilon_i-\varepsilon_f)[1 + (\alpha\sigma)^n]^{-m} \qquad (2)$$

Where ε_i is the void rate of the sample without load application; ε_f is the final void rate of the sample, for this study this value was estimated as an adjustment parameter; α, n and m are parameters of adjustment, imposing the restriction $m = 1 - 1/n$.

Models of soil load support capacity (MSLSC) were obtained fitting σ_P (kPa) to bulk density (Mg m^{-3}) and water content (kg kg^{-1}) using a non-linear model adapted from Busscher (1990) (Eq. (3)) for each soil tillage system irrespective of the cropping systems.

$$\sigma_P = aBD^bW^C \qquad (3)$$

where σ_P is the soil load support capacity; BD is the bulk density; W is the soil gravimetric water content; a, b and c are fitting parameters of the model.

2.4. Data analysis

The MSLSCs (Eq. (3)) were fitted to the measured data using the routine "PROC NLIN" following the Gauss-Newton method from the Statistical Analysis System 8.0 (SAS 8.0), and the graphs plotted through the program SigmaPlot®12.5 (*Systat software, Inc.*). Adjusted σ_p values were subjected to analysis of variance (ANOVA) using the software SAS 8.0, with significant differences reported at $p < 0.05$. Independently of soil layers, the MSLSCs were compared among soil tillage systems using the area under the curve, calculated by the integral of the adjusted Eq. (3), considering water content and bulk density values ranging from 0.26 to 0.35 kg kg^{-1} and 1.05 to 1.32 Mg m^{-3}, respectively. These intervals were chosen to comprise the common values for all treatments at field condition. Areas under the curves were calculated with numerical integration considering the portions based on Vectorized adaptive quadrature (quadva) routine (Shampine, 2008) using the Matlab® software, thus, the integral values were subjected to ANOVA test ($p < 0.05$). Whenever F-values were significant ($p < 0.05$), means were compared by Tukey test ($p < 0.05$) using the Minitab® 18.1 software.

2.5. Statistical evaluation of model performance

The agreement between simulated and measured values was expressed by the mean absolute error (MAE) (Eq. (4)) (Casaroli et al., 2010), the root-mean-squared error (RMSE) (Eq. (5)) (de Jong van Lier et al., 2008), the coefficient of residual mass (CRM) (Eq. (6)), the coefficient of correlation (r) (Eq. (7)) (Bonfante et al., 2010), and the index of agreement (d) (Eq. (8)) (Casaroli et al., 2010). Also, the modelling efficiency (EF) (Eq. (9)) (Bonfante et al., 2010) was used as criteria to evaluate the model performance. In the graph of observed and measured values, the 1:1 line was plotted for reference (Willmott et al., 2012).

$$MAE = \frac{1}{n}\sum_{i=1}^{n} |P_i-O_i| \qquad (4)$$

where n is the total number of measurements, O_i and P_i are the measured and predicted values of the observation, respectively. In an ideal case, the root-mean-square error (RMSE) has minimum value of zero. It is a difference-based measure of the model performance in a quadratic form, and it is sensitive to outliers.

$$RMSE = \sqrt{\frac{1}{n}\sum_{i=1}^{n} (P_i-O_i)^2} \qquad (5)$$

The coefficient of residual mass (CRM) ranges between $-\infty$ and $+\infty$, with the optimum equal to zero. Positive values indicate that the

model underestimates the prediction, and negative values indicate overestimation. When CRM is close to zero it indicates no trends.

$$CRM = \frac{\sum_{i=1}^{n} Oi- \sum_{i=1}^{n} Pi}{\sum_{i=1}^{n} Oi} \qquad (6)$$

The optimum value of the coefficient of correlation (r) (Addiscott and Whitmore, 1987) is equal to $\pm$ 1; zero means no correlation.

$$r = \frac{\sigma OP}{\sigma O.\ \sigma P} \qquad (7)$$

where σOP is the covariance between measured and estimated data and σO and σP are the measured and estimated standard deviation, respectively.

The index of agreement of Willmott (d) is dimensionless, lies between -1.0 and 1.0, and is mostly related to model accuracy rather than other indices (Willmott et al., 2012).

$$d = 1-\frac{\sum_{i=1}^{n} (P_i-Oi)^2}{\sum_{i=1}^{n} (|P_i-\bar{O}| + |Oi-\bar{O}|)^2} \qquad (8)$$

Modelling efficiency (EF) (Greenwood et al., 1985) can be either positive or negative, 1 being the maximum limit, while negative infinity is the theoretical lowest boundary. EF values lower than 0 result from a worse fit rather than the average of measurements.

$$EF = \frac{\sum_{i=1}^{n} (O_i-\bar{O})^2-\sum_{i=1}^{n} (P_i-O_i)^2}{\sum_{i=1}^{n} (O_i-\bar{O})^2} \qquad (9)$$

3. Results and discussion

Soil parameters for soil load support capacity modelling are presented in Table 1. All tillage systems showed a wide range of bulk density and water content values (Table 1). The wider range was observed at 0.0-0.10 m depth, reflecting the horizontal soil variability induced mainly by spatial variations of soil disturbance, machinery

Table 1

Descriptive statistics of soil properties of a Rhodic Eutrudox under tillage systems at three soil layers.

Parameter	Soil layer (m)								
	0.0-0.10			0.10-0.20			0.20-0.30		
	Mean	Min.	Max.	Mean	Min.	Max.	Mean	Min.	Max.
				CT					
BD	1.13	0.87	1.40	1.31	1.17	1.42	1.32	1.23	1.42
W	0.28	0.22	0.35	0.30	0.25	0.34	0.31	0.26	0.36
σ_p	184	41	400	263	96	479	283	188	388
				MTC$_1$					
BD	1.18	1.02	1.36	1.28	1.17	1.43	1.27	1.12	1.37
W	0.29	0.23	0.34	0.31	0.26	0.35	0.31	0.26	0.35
σ_p	205	72	385	299	83	583	326	61	583
				MTC$_3$					
BD	1.17	0.99	1.35	1.31	1.21	1.37	1.28	1.20	1.33
W	0.29	0.23	0.35	0.30	0.24	0.35	0.32	0.27	0.35
σ_p	256	86	558	383	122	723	362	143	720
				NT$_{11}$					
BD	1.27	1.05	1.45	1.34	1.24	1.42	1.32	1.25	1.38
W	0.29	0.22	0.34	0.29	0.23	0.33	0.30	0.26	0.34
σ_p	331	68	618	381	119	611	451	126	1060
				NT$_{24}$					
BD	1.18	0.86	1.39	1.32	1.26	1.38	1.28	1.15	1.33
W	0.30	0.25	0.35	0.30	0.26	0.34	0.32	0.28	0.36
σ_p	290	58	607	459	235	820	400	164	811

CT: conventional tillage; MTC$_1$: minimum tillage with chiselling every year; MTC$_3$: minimum tillage with chiselling every 3 year; NT$_{11}$: continuous no-tillage for 11 years; NT$_{24}$: continuous no-tillage for 24 years. BD: bulk density (Mg m^{-3}); W: soil gravimetric water content (kg kg^{-1}); σ_p: preconsolidation pressure (kPa). Min: minimum; Max: maximum.

Table 2

Empirical parameters fitted to the models of soil load support capacity (σ_p = a*BD^b*W^c) for tillage systems in a Rhodic Eutrudox.

Parameter	Value	Standard error	Confidence interval		R^2
			CT		
a	36.29	16.47	3.43	69.16	
b	2.45	0.45	1.56	3.34	0.92*
c	−1.09	0.33	−1.75	−0.43	
			MTC_1		
a	3.17	2.59	−1.99	8.34	
b	3.99	0.91	2.17	5.81	0.85*
c	−2.94	0.54	−4.02	−1.86	
			MTC_3		
a	4.04	1.93	0.184	7.89	
b	3.82	0.70	2.419	5.22	0.89*
c	−2.94	0.34	−3.63	−2.25	
			NT_{11}		
a	5.26	3.03	−0.80	11.31	
b	2.59	0.83	0.93	4.25	0.89*
c	−2.89	0.37	−3.64	−2.15	
			NT_{24}		
a	3.52	1.75	0.03	7.01	
b	3.42	0.60	2.23	4.61	0.93*
c	−3.25	0.35	−3.95	−2.54	

CT: conventional tillage; MTC_1: minimum tillage with chiselling every year; MTC_3: minimum tillage with chiselling every 3 years; NT_{11}: continuous no-tillage for 11 years; NT_{24}: continuous no-tillage for 24 years. R^2 = [1-(SQresidual/SQregression)]; BD: bulk density (Mg m^{-3}); W: soil gravimetric water content (kg kg^{-1}). *significant at 5% level of probability by F-test.

traffic intensity, and input of organic materials. In addition, MTC_1 showed large ranges of water content and bulk density in comparison with the other tillage systems, probably resulting from different degrees of soil disturbance associated with the sampling position in relation to the chisel plough shanks. The bulk density range reflects an intermediary soil compaction level, considering that the maximum bulk density for this soil was 1.5 Mg m^{-3} (Moraes et al., 2012).

The fitted parameters of MSLSCs for tillage systems at the soil profile are shown in Table 2. The models explained from 85% (MTC_1) to 93% (NT_{24}) of σ_p variability. Moreover, the MSLSCs were significant (p < 0.05) regardless of the tillage systems and layers. The high determination coefficients indicate that the Busscher model (Eq. (3)) is suitable to estimate σ_p from bulk density and soil water content for all tillage systems at all soil depths. The relation between measured and calculated soil load support capacity for all tillage systems are distributed closely around the one-to-one line (Fig. 1). Indicators describing the model quality were promising with a coefficient of residual mass (CRM) close to zero in all the treatments; modelling efficiency
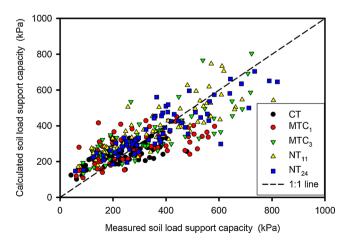
Table 3

Statistical evaluation of model performance of soil load support capacity in the tillage systems.

Model performance	Tillage systems				
	CT	MTC_1	MTC_3	NT_{11}	NT_{24}
RMSE	71.47	111.65	119.04	132.44	108.21
CRM	−0.0040	−0.0002	−0.0090	−0.0120	−0.0040
r	0.62	0.61	0.75	0.75	0.78
EF	0.40	0.38	0.58	0.56	0.63
d	0.74	0.73	0.84	0.82	0.87
MAE	59.07	88.42	93.95	100.05	78.02

RMSE: root-mean-square error; CRM: coefficient of residual mass; r: coefficient of correlation; EF: modelling efficiency; d: index of agreement; MAE: mean absolute error.

(EF) was up to 0.63 (NT_{24}); the index of agreement (d) ranged from 0.73 (MTC_1) to 0.87 (NT_{24}), where correlation coefficient (r) was from 0.61 (MTC_1) to 0.78 (NT_{24}) (Table 3). In addition, the determination coefficient of higher than 0.85 (MTC_1) (Table 2) and the confidence interval of the parameters b and c $\neq$ 0, indicate that all parameters were significant (Table 2). This suggests that the relevant effect of bulk density and water content were captured in the model to estimate the soil load support capacity in all tillage systems.

The σ_p range differed among tillage systems regardless of soil layers, as a result of differences in soil structure, bulk density and water content (Fig. 2). For the same bulk density and water content, σ_p usually increased with increasing the time after the last soil disturbance. For better understanding, we modelled σ_p as a function of bulk density and water content independently of the soil layer (Fig. 3).

The σ_p was plotted as a function of water content (from 0.26 to 0.35 kg kg^{-1}) and bulk density (from 1.05 to 1.32 Mg m^{-3}) for all tillage systems (Fig. 3) using the MSLSC parameters shown in Table 2. Accordingly, clear differences are observed among tillage systems regarding the exponential growth of σ_p in response to bulk density increase and water content reduction. The bulk density (from 1.05 to 1.32 Mg m^{-3}) and water content (from 0.26 to 0.35 kg kg^{-1}) ranges were chosen because these values were observed in all soil layers and tillage systems in the field (Table 1). Moreover, plotting the MSLSC using the same bulk density and water content ranges (Fig. 3) allowed reliable comparisons among the treatments through the area under the curve - AUC (i.e. integral of the equation) (Table 4). The AUC represents the sum of the effect of bulk density and water content on the soil load support capacity in the ranges analysed. Thus, we used the AUC to compare results of the age-hardening phenomenon under different tillage systems using the soil load support capacity as a parameter to estimate the strengthening of the soil over the time.

The AUC for NT_{24} was greater than for the other tillage systems (Table 4). It is important to emphasize that AUC was usually higher in NT_{24} and NT_{11} in comparison with the every year chiselled treatment (MTC_1) in all soil profiles (Table 4), revealing that chiselling strongly reduced σ_p regardless of bulk density and water content. In addition, the integral of the model in MTC_1 was similar to that observed in conventional tillage, indicating that the use of chiselling or heavy disk can break the soil aggregates and result in reduced strength and soil load support capacity. Hence, chiselling increased the risk of soil compaction at all evaluated depths, explaining why several studies reporting short-lived effects of such tillage operation in tropical soils (e.g., Calonego and Rosolem, 2010; Moraes et al., 2016; Nunes et al., 2015). Lower σ_p in chiselled plots may be associated with the disruption of aggregates and bonds among soil particles, whose restoration may need long-term without soil mobilization (Fig. 4).

Considering the same bulk density and water content, σ_p values under NT_{24} were higher than NT_{11} in the entire soil profile, whereas they were higher under MTC_3 compared to MTC_1 indicating increment

Fig. 1. Measured vs. calculated values of soil load support capacity under different tillage systems in a very clayey, Rhodic Eutrudox. Dashed line represents a one-to-one relationship.
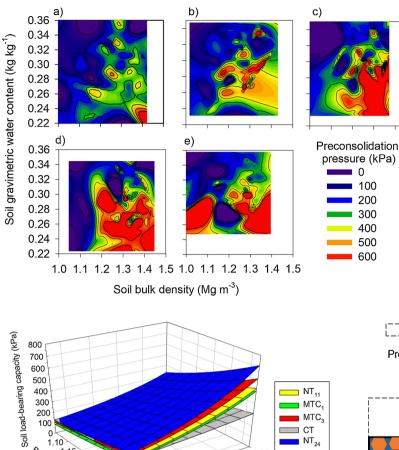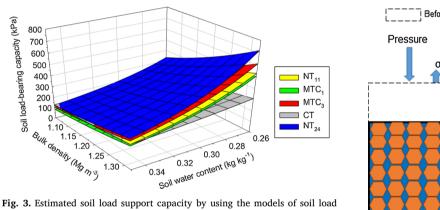
Fig. 2. Soil load support capacity (σ_p) affected by soil water content and bulk density, for different tillage systems in a Rhodic Eutrudox: CT (a); MTC$_1$ (b); MTC$_3$ (c); NT$_{11}$ (d); and NT$_{24}$ (e) CT: conventional tillage system; MTC$_1$: minimum tillage system chiselled every year; MTC$_3$: minimum tillage system chiselled every 3 years; NT$_{11}$: continuous no-tillage system for 11 years; NT$_{24}$: continuous no-tillage system for 24 years.

Fig. 3. Estimated soil load support capacity by using the models of soil load support capacity (MSLSC, Table 1) fitted for each tillage system, as a function of soil gravimetric water content and bulk density in a Rhodic Eutrudox in Londrina, PR, Brazil. NT$_{24}$: continuous no-tillage system for 24 years; NT$_{11}$: continuous no-tillage system for 11 years; MTC$_1$: minimum tillage system chiselled every year; MTC$_3$: minimum tillage system chiselled every 3 years; CT: conventional tillage system.

Fig. 4. Changes in the soil load support capacity (σp) over time in no-tillage system due to age-hardening phenomenon.

Table 4

Values of area under the curve of soil load support capacity at the range of bulk density and water content from tillage systems of a Rhodic Eutrudox.

Tillage systems	Area under the curve
CT	18.37c
MTC$_1$	19.89c
MTC$_3$	24.40b
NT$_{11}$	23.97b
NT$_{24}$	28.60a

[*]Means followed by the same letter did not differ at the 5% level of probability by Tukey test. CT: conventional tillage system; MTC$_1$: minimum tillage system with soil chiselling every year; MTC$_3$: minimum tillage system with soil chiselling every three years; NT$_{11}$: no-tillage continuous for 11 years; NT$_{24}$: no-tillage continuous for 24 years.

of soil strength over the time without soil mobilization, as shown by the AUC data (Table 4). For example, considering the same bulk density (1.20 Mg m^{-3}), when water content decreased from 0.35 to 0.26 kg kg^{-1}, σ_p increased from 175 to 415 kPa in NT$_{11}$, and from 198 to 520 kPa in
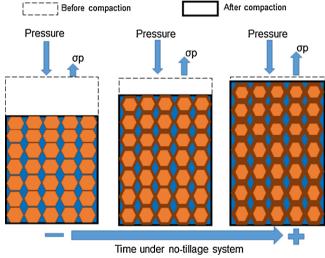
NT$_{24}$. These results emphasise that the soil strengthens over time after soil disturbance (Moraes et al., 2014), enabling the formation of stable aggregates (Moraes et al., 2017), and the formation of continuous pores within the soil profile (Reichert et al., 2016). Increased soil strength and hence σ_p over time after soil disturbance can be explained by soil resilience (Bonetti et al., 2017), and the age-hardening phenomena (Moraes et al., 2017). In addition, similar results were observed in the AUC values when comparing MTC$_1$ to MTC$_3$ revealing that a 3-year interval after chiselling was enough to detect significant increases in σ_p. Using that same example of bulk density of 1.20 Mg m^{-3}, the σ_p was reduced from 347 kPa (0.26 kg kg^{-1}) to 145 kPa (0.35 kg kg^{-1}) under MTC$_1$, while that value under MTC$_3$ changed from 425 kPa to 177 kPa. Both cases, indicate the strengthening of soil over time, emphasizing that restoring soil structure and strength in agricultural areas is a time-demanding, long-term process.

Considering the respective bulk density and water content under each of the management practices, soil load support capacity increased with time (Fig. 3). The effects of "cementation" among soil aggregates and particles are intensified with reduced water content and getting far from the field capacity (i.e., 0.34 kg kg^{-1} (Moraes et al., 2016)). Thus, soil load support capacity increased with time without chiselling (from

MTC_1 to MTC_3), when considering the same range of bulk density and water content (Fig. 3 and Table 4) for all soil layers. It indicates that soil chiselling weakens particle bonds, reduces soil load support capacity (Fig. 4), and emphasizes that every year chiselling can weaken the aggregates in the same way as conventional tillage (Table 4). Regardless of the mechanism involved, in the age-hardening process soil strength increases as a function of time without soil disturbance (Moraes et al., 2017). This process can also be considered as either the recovery of soil resistance with time by cohesion (Horn, 2004), or the reconstruction of the connections between soil particles broken due to soil disturbance with time (Błażejczak et al., 1995). Processes associated with physical degradation by soil mobilisation, may reduce the soil aggregation and strength (Veiga et al., 2007). The mechanisms involved in the age-hardening phenomena have been related to the rearrangement of soil particles via flocculation of clay particles accompanied by changes in pore size distribution and restoration of cementing bonds between soil particles, reflecting increase in tensile strength (Tormena et al., 2008).

Soil load support capacity is an important parameter for soil physical quality, directly related to soil structure (Ortigara et al., 2015) and the condition to root growth (Keller et al., 2015). This parameter is related to aggregate-tensile strength (Mosaddeghi et al., 2003), thus the age-hardening phenomenon (Moraes et al., 2017; Utomo and Dexter, 1981) could be evaluated by soil load support capacity to analyse the strengthening of soil structure. However, the soil load support capacity is affected by many soil parameters, particularly by soil structure, water content (Ortigara et al., 2015), and soil cohesion (Horn and Fleige, 2003). Soil cohesion is influenced by management systems and is associated with time, bulk density, water content (Kemper and Rosenau, 1984), organic carbon, and clay mineralogy, especially the contents of Fe, Si, and Al oxides in soil (Kemper et al., 1987). Soil structure affects the soil load support capacity defined as the maximum load per unit area the soil can support without additional compaction (Dias Junior and Pierce, 1995). Soil structure is very important as the risk of subsoil compaction is high when the exerted stresses are higher than the bearing capacity of the subsoil (Alakukku et al., 2003). Thus, our study showed that the soil load support capacity is influenced by soil tillage systems as a function of the age-hardening process at a certain bulk density and water content, revealing increases in soil cohesion due to the strengthening of existing inter-particle bonds as described for soil penetration resistance in short (Dexter et al., 1988) and long-term experiments (Moraes et al., 2017). This positive effect on soil load capacity was especially observed in the no-tillage system.

Soils under long-term no-tillage (NT_{24}) can support higher loads at a certain bulk density and water content, compared to the other tillage systems (minimum tillage) when subjected to mechanical pressures. This result indicates that in NT_{24}, more energy is needed to break the soil aggregates due to the greater soil strength as a consequence of strengthening of the bonds between particles and the cohesive forces of the soil (Wuddivira et al., 2013). The soil load support capacity has a direct relationship with aggregate tensile strength (Mosaddeghi et al., 2003). This higher stress pre-compression can be attributed directly to the absence of disturbance and indirectly to the accumulation of carbon in this layer for NT_{24} (21.9 g kg^{-1}) in relation to the other tillage systems [CT (18.9 g kg^{-1}), MTC_1 (19.9 g kg^{-1}), MTC_3 (19.8 g kg^{-1}) e NT_{11} (20.6 g kg^{-1})]. Avoiding soil disturbance increases soil strength due to strengthening of the existing bonds between soil aggregates (Moraes et al., 2017). A period of time after the establishment of a no-tillage system, an intense rearrangement of soil particles occurs during wetting and drying cycles (Reichert et al., 2016). In addition, no-tillage favours the formation of environments with greater biological diversity (Silva et al., 2014) and more root exudates (Rasse et al., 2005), which are important cohesive agents (Kemper et al., 1987). Thus, in clayey soils, where the area of contact between the particles is larger, the soil can support more loads under no-tillage system.

Soil mobilization breaks soil pore continuity, favouring the breakage of the existing bonds between the particles due the use of heavy harrowing (CT) and reduces the cohesion between soil particles (Moraes et al., 2017) that is detected by the reduction of pre-consolidation pressure throughout the soil profile (Fig. 3). The effect of heavy harrowing on soil degradation is intensified in the entire soil profile, for example, in the top soil layer, bulk density was reduced and resulted in decreased soil load support capacity (Fig. 3) and increased risk of soil erosion (Merten et al., 2015), while in the deeper soil layer, soil compaction forms a harrow pan (Moraes et al., 2016) without increments of soil load support capacity (Fig. 3). That means soil mobilization changes the soil structure, causes soil disaggregation and makes the particle bonds very weak (Moraes et al., 2017). Agricultural practices break the existing connections between the aggregates and weaken the structural stability of the soil favouring the soil re-compaction after agricultural machinery in areas with soil mobilization (Moraes et al., 2013). Therefore, when the soil is mobilized by soil chiselling, the negative effects on soil structure can last for a shorter time and be eliminated soon after the traffic or by the soil re-consolidation itself (Moraes et al., 2016).

In that way, soil load support capacity in no-tillage is increased in long-term due to the increment of soil cohesion (Kemper and Rosenau, 1984), revealing a cementation process strengthening the soil structure (Moraes et al., 2017). In addition, it was observed that load bearing capacity under NT_{11} was less than NT_{24} which is related to the process of age-hardening (Dexter et al., 1988) resulting in a higher accumulation of soil organic carbon under NT_{24} (21.9 g kg^{-1}) compared to NT_{11} (20.6 g kg^{-1}) (Moraes et al., 2017) and a longer period of time under no-tillage in NT_{24}.

4. Conclusions

No-tillage over two decades (NT_{24}) induced higher soil load support capacity (preconsolidation pressure) at a certain bulk density and water content compared to the other tillage systems (CT, MTC_1, MTC_3 and NT_{11}), evidencing the effects of the age-hardening processes.

The age-hardening phenomenon in the soil load support capacity can occur in an Oxisol under tillage systems as a function of time under no-tillage system, or with increasing time without soil chiselling.

Soil load support capacity increases as a function of time under no-tillage, improving the soil structure to support more pressure; while the soil structure under chiselling is negatively and strongly affected by soil mobilization which results in breaking particle bonds leading to greater soil compaction.

References

Addiscott, T.M., Whitmore, A.P., 1987. Computer simulation of changes in soil mineral nitrogen and crop nitrogen during autumn, winter and spring. J. Agric. Sci. 109, 141. https://doi.org/10.1017/S0021859600081089.

Alakukku, L., Weisskopf, P., Chamen, W.C.T., Tijink, F.G.J., van der Linden, J.P., Pires, S., Sommer, C., Spoor, G., 2003. Prevention strategies for field traffic-induced subsoil compaction: a review. Soil Tillage Res. 73, 145–160. https://doi.org/10.1016/S0167-1987(03)00107-7.

Alvares, C.A., Stape, J.L., Sentelhas, P.C., de Moraes Gonçalves, J.L., Sparovek, G., 2013. Köppen's climate classification map for Brazil. Meteorol. Zeitschrift 22, 711–728. https://doi.org/10.1127/0941-2948/2013/0507.

Assouline, S., 2002. Modeling soil compaction under uniaxial compression. Soil Sci. Soc. Am. J. 66, 1784. https://doi.org/10.2136/sssaj2002.1784.

Baumgartl, T., Kock, B., 2004. Modeling volume change and mechanical properties with hydraulic models. Soil Sci. Soc. Am. J. 68, 57–65. https://doi.org/10.2136/sssaj2004.5700.

Blake, G.R., Hartge, K.H., 1986a. Bulk density. In: Klute, A. (Ed.), Methods of Soil Analysis: Part 1 Physical and Mineralogical Methods. American Society of Agronomy, Madison, pp. 363–376.

Blake, G.R., Hartge, K.H., 1986b. Particle density. In: Klute, A. (Ed.), Methods of Soil Analysis: Part 1 Physical and Mineralogical Methods. American Society of Agronomy, Madison, pp. 377–382.

Błażejczak, D., Horn, R., Pytka, J., Btazejczak, D., Horn, R., Pytka, J., 1995. Soil tensile strength as affected by time, water content and bulk density. Int. Agrophys. 9, 179–188.

Bonfante, A., Basile, A., Acutis, M., De Mascellis, R., Manna, P., Perego, A., Terribile, F., 2010. SWAP, CropSyst and MACRO comparison in two contrasting soils cropped with maize in Northern Italy. Agric. Water Manag. 97, 1051–1062. https://doi.org/10.1016/j.agwat.2010.02.010.

Busscher, W.J., 1990. Adjustment of flat-tipped penetrometer resistance data to a common water content. Trans. ASAE 33, 0519–0524. https://doi.org/10.13031/2013.31360.

Calonego, J.C., Rosolem, C.A., 2010. Soybean root growth and yield in rotation with cover crops under chiseling and no-till. Eur. J. Agron. 33, 242–249. https://doi.org/10.1016/j.eja.2010.06.002.

Casagrande, A., 1936. The determination of pre-consolidation load and its practical significance. Proceedings 1st International Conference on Soil Mechanics and Foundation Engineering. pp. 60–64.

Casaroli, D., de Jong van Lier, Q., Dourado Neto, D., 2010. Validation of a root water uptake model to estimate transpiration constraints. Agric. Water Manag. 97, 1382–1388. https://doi.org/10.1016/j.agwat.2010.04.004.

Silva, R.B., Lanças, K.P., Junior Masquetto, B., 2007. Consolidometer: electronic-pneumatic equipament to evaluate soil consolidation. Rev. Bras. Ciência do Solo 31, 607–615. https://doi.org/10.1590/S0100-06832007000400001.

Silva, A.P., Babujia, L.C., Franchini, J.C., Ralisch, R., Hungria, M., de F. Guimarães, M., 2014. Soil structure and its influence on microbial biomass in different soil and crop management systems. Soil Tillage Res. 142, 42–53. https://doi.org/10.1016/j.still.2014.04.006.

Veiga, M., Horn, R., Reinert, D.J., Reichert, J.M., 2007. Soil compressibility and penetrability of an Oxisol from southern Brazil, as affected by long-term tillage systems. Soil Tillage Res. 92, 104–113. https://doi.org/10.1016/j.still.2006.01.008.

Bonetti, J.A., Anghinoni, I., Moraes, M.T., Fink, J.R., 2017. Resilience of soils with different texture, mineralogy and organic matter under long-term conservation systems. Soil Tillage Res. 174, 104–112. https://doi.org/10.1016/j.still.2017.06.008.

de Jong van Lier, Q., van Dam, J.C., Metselaar, K., de Jong, R., Duijnisveld, W.H.M., 2008. Macroscopic root water uptake distribution using a matric flux potential approach. Vadose Zone J. 7, 1065. https://doi.org/10.2136/vzj2007.0083.

Moraes, M.T., Debiasi, H., Franchini, J.C., Silva, V.R., 2012. Correction of resistance to penetration by pedofunctions and a reference soil water content. Rev. Bras. Ciência do Solo 36, 1704–1713. https://doi.org/10.1590/S0100-06832012000600004.

Moraes, M.T., Debiasi, H., Franchini, J.C., Silva, V.R., 2013. Soil penetration resistance in a rhodic eutrudox affected by machinery traffic and soil water content. Eng. Agrícola 33, 748–757. https://doi.org/10.1590/S0100-69162013000400014.

Moraes, M.T., Debiasi, H., Carlesso, R., Franchini, J.C., Silva, V.R., 2014. Critical limits of soil penetration resistance in a rhodic Eutrudox. Rev. Bras. Ciência do Solo 38, 288–298. https://doi.org/10.1590/S0100-06832014000100029.

Moraes, M.T., Debiasi, H., Carlesso, R., Franchini, J.C., Silva, V.R., Luz, F.B., 2016. Soil physical quality on tillage and cropping systems after two decades in the subtropical region of Brazil. Soil Tillage Res. 155, 351–362. https://doi.org/10.1016/j.still.2015.07.015.

Moraes, M.T., Debiasi, H., Carlesso, R., Franchini, J.C., Silva, V.R., Luz, F.B., 2017. Age-hardening phenomena in an oxisol from the subtropical region of Brazil. Soil Tillage Res. 170, 27–37. https://doi.org/10.1016/j.still.2017.03.002.

Dexter, A.R., Horn, R., Kemper, W.D., 1988. Two mechanisms for age-hardening of soil. J. Soil Sci. 39, 163–175. https://doi.org/10.1111/j.1365-2389.1988.tb01203.x.

Dias Junior, M.S., Pierce, F.J., 1995. A simple procedure for estimating preconsolidation pressure from soil compression curves. Soil Technol. 8, 139–151. https://doi.org/10.1016/0933-3630(95)00015-8.

Franchini, J.C., Debiasi, H., Balbinot Junior, A.A., Tonon, B.C., Farias, J.R.B., de Oliveira, M.C.N., Torres, E., 2012. Evolution of crop yields in different tillage and cropping systems over two decades in southern Brazil. F. Crop. Res. 137, 178–185. https://doi.org/10.1016/j.fcr.2012.09.003.

Greenwood, D.J., Neeteson, J.J., Draycott, A., 1985. Response of potatoes to N fertilizer: dynamic model. Plant Soil 85, 185–203. https://doi.org/10.1007/BF02139623.

Gubiani, P.I., Reinert, D.J., Reichert, J.M., Goulart, R.Z., Fontanela, E., 2017. Excel ADD-IN to model the soil compression curve. Eng. Agrícola 37, 603–610. https://doi.org/10.1590/1809-4430-eng.agric.v37n3p603-610/2017.

Horn, R., 2004. Time dependence of soil mechanical properties and pore functions for arable soils. Soil Sci. Soc. Am. J. 68, 1131. https://doi.org/10.2136/sssaj2004.1131.

Horn, R., Fleige, H., 2003. A method for assessing the impact of load on mechanical stability and on physical properties of soils. Soil Tillage Res. 73, 89–99. https://doi.org/10.1016/S0167-1987(03)00102-8.

Imhoff, S., Pires da Silva, A., Ghiberto, P.J., Tormena, C.A., Pilatti, M.A., Libardi, P.L., 2016. Physical quality indicators and mechanical behavior of agricultural soils of Argentina. PLoS One 11, e0153827. https://doi.org/10.1371/journal.pone.0153827.

Keller, T., Lamandé, M., 2010. Challenges in the development of analytical soil compaction models. Soil Tillage Res. 111, 54–64. https://doi.org/10.1016/j.still.2010.08.004.

Keller, T., Silva, A.P., Tormena, C.A., Giarola, N.F.B., Cavalieri, K.M.V., Stettler, M., Arvidsson, J., 2015. SoilFlex-LLWR: linking a soil compaction model with the least limiting water range concept. Soil Use Manag. 31, 321–329. https://doi.org/10.1111/sum.12175.

Kemper, W.D., Rosenau, R.C., 1984. Soil cohesion as affected by time and water content. Soil Sci. Soc. Am. J. 48, 1001. https://doi.org/10.2136/sssaj1984.03615995004800050009x.

Kemper, W.D., Rosenau, R.C., Dexter, a.R., 1987. Cohesion development in disrupted soils as affected by clay and organic matter content and temperature1. Soil Sci. Soc. Am. J. 51, 860. https://doi.org/10.2136/sssaj1987.03615995005100040004x.

Mazurana, M., Levien, R., Inda Junior, A.V., Conte, O., Bressani, L.A., Müller, J., 2017. Soil susceptibility to compaction under use conditions in southern Brazil. Ciência e Agrotecnologia 41, 60–71. https://doi.org/10.1590/1413-70542017411027216.

Merten, G.H., Araújo, A.G., Biscaia, R.C.M., Barbosa, G.M.C., Conte, O., 2015. No-till surface runoff and soil losses in southern Brazil. Soil Tillage Res. 152, 85–93. https://doi.org/10.1016/j.still.2015.03.014.

Mosaddeghi, M., Hemmat, A., Hajabbasi, M.A., Alexandrou, A., 2003. Pre-compression stress and its relation with the physical and mechanical properties of a structurally unstable soil in central Iran. Soil Tillage Res. 70, 53–64. https://doi.org/10.1016/S0167-1987(02)00120-4.

Nunes, M.R., Denardin, J.E., Pauletto, E.A., Faganello, A., Pinto, L.F.S., 2015. Effect of soil chiseling on soil structure and root growth for a clayey soil under no-tillage. Geoderma 259–260, 149–155. https://doi.org/10.1016/j.geoderma.2015.06.003.

Ortigara, C., Moraes, M.T., Debiasi, H., Silva, V.R., Franchini, J.C., Luz, F.B., 2015. Modeling of soil load-bearing capacity as a function of soil mechanical resistance to penetration. Rev. Bras. Ciência do Solo 39, 1036–1047. https://doi.org/10.1590/01000683rbcs20140732.

Pires, L.F., Borges, J.A.R., Rosa, J.A., Cooper, M., Heck, R.J., Passoni, S., Roque, W.L., 2017. Soil structure changes induced by tillage systems. Soil Tillage Res. 165, 66–79. https://doi.org/10.1016/j.still.2016.07.010.

Rasse, D.P., Rumpel, C., Dignac, M.-F., 2005. Is soil carbon mostly root carbon? Mechanisms for a specific stabilisation. Plant Soil 269, 341–356. https://doi.org/10.1007/s11104-004-0907-y.

Reichert, J.M., Rosa, V.T., Vogelmann, E.S., Rosa, D.P., Horn, R., Reinert, D.J., Sattler, A., Denardin, J.E., 2016. Conceptual framework for capacity and intensity physical soil properties affected by short and long-term (14 years) continuous no-tillage and controlled traffic. Soil Tillage Res. 158, 123–136. https://doi.org/10.1016/j.still.2015.11.010.

Santos, H.G., Jacomine, P.K.T., Anjos, L.H.C., Oliveira, V.A., Lubreras, J.F., Coelho, M.R., Almeida, J.A., Cunha, T.J.F., Oliveira, J.B., 2013. Sistema brasileiro de classificação de Solos, 3ª. ed. Embrapa, Brasília.

Shampine, L.F., 2008. Vectorized adaptive quadrature in MATLAB. J. Comput. Appl. Math. 211, 131–140. https://doi.org/10.1016/j.cam.2006.11.021.

Silva, V.R., Reinert, D.J., Reichert, J.M., 2000. Susceptibility to compaction of a Haplortox and a Paleudalf. Rev. Bras. Ciências do Solo 24, 239–249. https://doi.org/10.1590/S0100-06832000000200001.

Soil Survey Staff, 2014. Keys to soil taxonomy. Soil Conservation Service, 12th ed. USDA-Natural Resources Conservation Service, Washington, DC.

Tang, A.-M., Cui, Y.-J., Eslami, J., Défossez, P., 2009. Analysing the form of the confined uniaxial compression curve of various soils. Geoderma 148, 282–290. https://doi.org/10.1016/j.geoderma.2008.10.012.

Tormena, C.A., Fidalski, J., Rossi Junior, W., 2008. Resistência tênsil e friabilidade de um Latossolo sob diferentes sistemas de uso. Rev. Bras. Ciência do Solo 32, 33–42. https://doi.org/10.1590/S0100-06832008000100004.

Utomo, W.H., Dexter, A.R., 1981. Age hardening of agricultural top soils. J. Soil Sci. 32, 335–350. https://doi.org/10.1111/j.1365-2389.1981.tb01710.x.

van Genuchten, M.T., 1980. A closed-form equation for predicting the hydraulic conductivity of unsaturated soils. Soil Sci. Soc. Am. J. 44, 892–898. https://doi.org/10.2136/sssaj1980.03615995004400050002x.

Veenhof, D.W., McBride, R.A., 1996. Overconsolidation in agricultural soils: I. Compression and consolidation behavior of remolded and structured soils. Soil Sci. Soc. Am. J. 60, 362. https://doi.org/10.2136/sssaj1996.03615995006000020006x.

Willmott, C.J., Robeson, S.M., Matsuura, K., 2012. A refined index of model performance. Int. J. Climatol. 32, 2088–2094. https://doi.org/10.1002/joc.2419.

Wuddivira, M.N., Stone, R.J., Ekwue, E.I., 2013. Influence of cohesive and disruptive forces on strength and erodibility of tropical soils. Soil Tillage Res. 133, 40–48. https://doi.org/10.1016/j.still.2013.05.012.